Journal of Research in Medical and Dental Science
2018, Volume 6, Issue 4, Page No: 24-29

Available Online at: www.jrmds.in
eISSN No. 2347-2367: pISSN No. 2347-2545

CT Evaluation of the Intraorbital Structures Concerning Endoscopic Approaches to the Lamina Papyracea

Gülay Açar[1*], Mustafa Büyükmumcu[1], İbrahim Güler[2]

[1]Department of Anatomy, Faculty of Medicine, Necmettin Erbakan University, Meram, Konya, Turkey
[2]Department of Radiology, Faculty of Medicine, Selçuk University, Selçuklu, Konya, Turkey

ABSTRACT

Background: The relationship between the intraorbital structures and medial wall of the orbit is essential for surgical approaches.
Objective: The goal was to provide an improved understanding of the dimensions of extraocular muscles and the approximate location of the intraorbital structures with respect to the lamina papyracea (LP).
Material and Methods: This retrospective study was performed using the multiplanar reconstruction of Computed Tomography (CT) scans of 200 orbits.
Results: We measured the mean diameters of intraorbital structures. The mean horizontal distances from LP to medial and inferior rectus muscles, globe, and infraorbital canal were found as 3.9 ± 1.2 mm, 11.5 ± 1.6 mm, 7.8 ± 1.5 mm and 16.1 ± 2.0 mm and as 0.6 ± 0.4 mm, 4.7 ± 1.3 mm, 7.2 ± 1.8 mm, 12.5 ± 2.3 mm at the depth of the anterior (AEF) and posterior ethmoidal foramen, respectively. All morphometric results were compared with respect to age, sex and laterality and higher in males than females. The measurement results indicated that subjects in first and second age groups showed statistically significant differences in distances from the LP to the globe, medial and inferior rectus muscles at the depth of AEF ($p<0.05$). But, there was no difference between right and left.
Conclusion: CT imaging which can offer an accurate understanding of the regional anatomy of and around the LP may be helpful in preoperative planning and prediction of postoperative outcomes. It can allow the surgeon to prevent possible orbital injury during surgical interventions.

Key words: Computed tomography, The diameter of the extraocular muscle, Endoscopic approach, Intraorbital structures, Lamina papyracea

HOW TO CITE THIS ARTICLE: Gülay Açar*, Mustafa Büyükmumcu, İbrahim Güler, CT evaluation of the intraorbital structures concerning endoscopic approaches to the lamina papyracea, J Res Med Dent Sci, 2018, 6 (4):24-29

Corresponding author: Gülay Açar
e-mail✉: gulayzeynep73@gmail.com
Received: 14/06/2018
Accepted: 13/07/2018

INTRODUCTION

Much orbital pathology including neoplasm, vascular malformation, trauma, acromegaly and Graves' orbitopathy alter the diameters of the extraocular muscles and the volume of the orbital cavity [1]. The difference between diameters of healthy and Graves' extraocular muscles is essential in orbital pathology diagnosis, treatment and outcome prediction. Especially, the treatment of primary or metastatic tumors of orbit, which represent less than 1% of the head and neck tumors requires a surgical approach [1,2]. During surgical interventions, orbital complications including orbital penetration, periorbital hematoma and emphysema, diplopia, nasolacrimal duct injury, and iatrogenic optic nerve injury can occur because of the orbit and paranasal sinuses are in close proximity [3-6].

The lamina papyracea (LP), which shares a boundary with the paranasal structures, is extremely thin and the weakest part of the medial wall providing the least resistance to surgical interventions like endoscopic sinus surgery, orbital reconstruction, and decompression surgery. The anterior (AEF) and posterior ethmoidal (PEF) foramina, through which the anterior and posterior ethmoidal arteries pass, localize at the level of the frontoethmoidal suture forming the upper boundary of the medial wall of the orbit [7-9]. Because of this region have complex anatomy with variations of the neurovascular structures, a thorough study of the anatomical landmarks on LP and its relationships with the intraorbital structures is essential to perform an endoscopic endonasal approach (EEA) [10-12]. The EEA provides an excellent magnification and angled visualization. It allows surgeons to reach the retrobulbar medial and inferior parts, and also orbital apex. Also, it provides a confident surgical corridor for the resection of pathology which located in the compartment between

the medial (MRM) and inferior rectus muscles (IRM) [3,6,7,13,14].

The imaging techniques to evaluate the intraorbital structures such as ultrasound, computed tomography (CT) and magnetic resonance imaging (MRI) have been widely used. Especially, by using the multiplanar reconstruction (MPR) the detailed knowledge of the normal anatomy of the orbital cavity, the spatial relationship of the intraorbital structures with orbital wall and CT volume measurements, which is essential for surgical orbital decompression can be acquired [15,16].

In our study, we measured a set of linear parameters to describe the morphology of the orbital muscles and the exact position of the intraorbital structures with respect to the LP concerning surgical approaches. The measurements of these distances and the diameters of muscles may serve as crucial clinical applications for meticulous planning, localizing the ethmoidal foramina where bleeding occurs, and predicting outcomes. We aimed to show the approximate diameter and location of the intraorbital structures related with the LP that can prevent the iatrogenic complications and increase the success rate of surgery.

MATERIAL AND METHODS

We evaluated paranasal Multidetector CT images of 100 patients, ranging from 18 to 90 years of age, who appealed to the Department of Radiology for clinical purposes between September 2015 and July 2016. This retrospective study was approved by the Necmettin Erbakan University Ethics Committee with an approval number 2016/539. All patients were evaluated using 128-slice CT scanner (Siemens, imaging parameters: 120 kV; 160 mA; rotation time 0.5 s; collimation 128 × 0.625; FOV 220 mm). Axial CT images which were acquired with a section thickening of 0.625 mm were used to get associated coronal and sagittal images of 1 mm thickness. Images were analyzed by two investigators in a team (a radiologist and an anatomist) at a workstation (Syngo Via, Siemens, Germany). Also, they measured all parameters twice on each side and the mean value was used for statistical analysis. The patients who had orbital fractures, congenital deformities and with any distorting pathologies, which damaged the orbital bony contours and volume were excluded.

All of the linear parameters were identified in Table 1. We measured the diameters of extraocular muscles and optic nerve (ON) at 1 cm posterior to the globe (G) in the coronal plane, which the crista galli appeared (Figure 1).

Table 1: Definition of measurements of the orbital morphometry

Measurements	Definitions
Extraocular muscles diameters (1 cm posterior to the globe)	
MR, LR and SO muscles	The horizontal diameters of medial, lateral rectus and superior obliq muscles in coronal plane
SR and IR muscles	The vertical diameters of superior and inferior rectus muscles in coronal plane
ON diameter	The horizontal diameter of the optic nerve in coronal plane
ON length	The length of intraorbital optic nerve from the optic foramen to the globe in axial plane
At the depth of anterior ethmoidal foramen	
LP-MRM Distance	The distance from the lamina papyracea to the medial rectus muscle
LP-G Distance	The distance from the lamina papyracea to the globe
LP-IRM Distance	The distance from the lamina papyracea to the inferior rectus muscle
LP-IOC Distance	The distance from the lamina papyracea to the infraorbital canal
At the depth of posterior ethmoidal foramen	
LP-MRM Distance	The distance from the lamina papyracea to the medial rectus muscle
LP-G Distance	The distance from the lamina papyracea to the globe
LP-IRM Distance	The distance from the lamina papyracea to the inferior rectus muscle
LP-IOC Distance	The distance from the lamina papyracea to the infraorbital canal

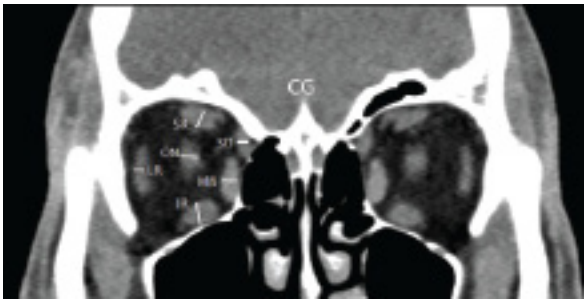

Figure 1: Measurements regarding the extraocular muscles and optic nerve diameters (white lines) in coronal plane (MR: medial rectus, IR: inferior rectus, LR: lateral rectus, SR: superior rectus, SO: superior oblique, ON: optic nerve, CG: crista galli)

Also, the length of the intraorbital ON was measured in the axial plane. To evaluate the relationship between the intraorbital structures and medial orbital wall, the mean distances from the LP to MRM, IRM, ON, G and infraorbital canal (IOC) were measured separately in the coronal planes at the depth of the AEF and PEF. Through multiplanar reconstructions, in separate axial planes, the AEF and PEF were identified by locating the intersection of x and y-axes at the AEF and PEF (Figures 2A and 3A).

Then, in the coronal plane that was equivalent to the position of the AEF the vertical axis was passed along the LP and the distances from the LP to MRM, IRM, G and IOC were measured (Figure 2B). Similarly, in coronal plane that was equivalent to the position of the PEF the vertical axis was passed along the LP and the distances from the LP to MRM, IRM, ON, and IOC were measured (Figure 3B).

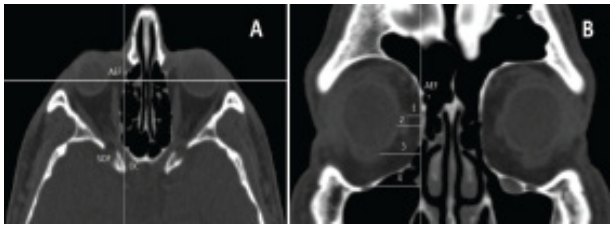

Figure 2: Measurements between lamina papyracea and intraorbital structures at the depth of the anterior ethmoidal foramen (AEF). [A] The intersection of x and y axes were located at

the AEF in axial plane, SOF: superior orbital fissure, OC: optic canal. [B] The horizontal distances (white lines) from the medial wall to medial (1) and inferior rectus muscle (3), globe (2), infraorbital canal (4).

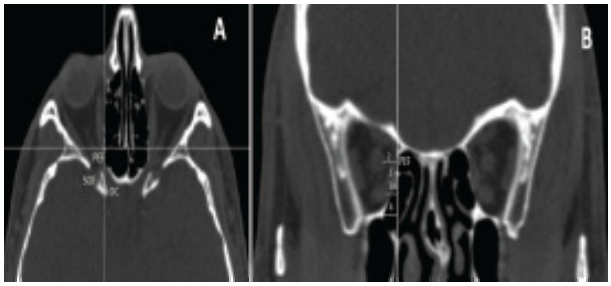

Figure 3: Measurements between lamina papyracea and intraorbital structures at the depth of the posterior ethmoidal foramen (PEF). [A] The intersection of x and y axes were located at the PEF in axial plane, SOF: superior orbital fissure, OC: optic canal. [B] The horizontal distances (white lines) from the medial wall to medial (1) and inferior rectus muscle (3), optic nerve (2), infraorbital canal (4).

On the other hand, we compared the mean measurement values within 3 age groups and by gender as well as on the left and right sides. The analyses with respect to sex, age and laterality were shown in Tables 2-4.

SPSS 22 (SPSS, Inc., Chicago, IL, USA) was used for statistical analysis. For statistical comparisons, Chi-square test, T-test, One-Way Analysis of Variance (ANOVA) were used. A value of $p<0.05$ was considered significant.

Table 2: The distribution of the comparison in morphometric measurements between females and males

Extraocular muscles diameters (mm)	Female	Male	Total	p value
	Mean ± SD	Mean ± SD	Mean ± SD	
MRM	3.7 ± 0.5	3.9 ± 0.5	3.9 ± 0.5	0.04
IRM	3.8 ± 0.6	4.2 ± 0.6	4.1 ± 0.6	0.002
LRM	2.3 ± 0.4	2.5 ± 0.5	2.5 ± 0.5	0.004
SRM	3.7 ± 0.6	4.2 ± 0.6	4.0 ± 0.6	<0.001
SOM	2.3 ± 0.6	2.7 ± 0.4	2.6 ± 0.5	<0.001
ON diameter	5.2 ± 0.4	5.3 ± 0.4	5.3 ± 0.4	0.131
ON length	27.2 ± 2.7	27.6 ± 2.1	27.5 ± 2.2	0.381
Anterior ethmoidal foramen				
LP-MRM	3.7 ± 0.9	3.9 ± 1.2	3.9 ± 1.2	0.126
LP-G	7.8 ± 1.7	7.8 ± 1.4	7.8 ± 1.5	0.877
LP-IRM	11.6 ± 1.6	11.5 ± 1.6	11.5 ± 1.6	0.609
LP-IOC	16.0 ± 2	16.2 ± 2	16.1 ± 2	0.64
Posterior ethmoidal foramen				
LP-MRM	0.5 ± 0.3	0.6 ± 0.4	0.6 ± 0.4	0.5
LP-ON	7.0 ± 1.6	7.3 ± 1.8	7.2 ± 1.8	0.46
LP-IRM	4.6 ± 1.1	4.8 ± 1.3	4.7 ± 1.3	0.46
LP-IOC	12.6 ± 2.2	12.4 ± 2.4	12.5 ± 2.3	0.586

MRM: medial rectus muscle, IRM: inferior rectus muscle, LRM: lateral rectus muscle, SRM: superior rectus muscle, SOM: superior oblique muscle, ON: optic nerve, LP: lamina papyracea, G: globe, IOC: infraorbital canal

Mean ± Standard Deviation.

Unpaired t test, $p<0.05$ shows statistically significant p values

Table 3: The distribution of the morphometric measurements with respect to age groups

Extraocular muscle diameters (mm)	(1) Age group (18-39 Y)	(2) Age group (40-59 Y)	(3) Age group (60-90 Y)
	Mean ± SD	Mean ± SD	Mean ± SD
MRM	3.6 ± 0.1*	4.0 ± 0.2*	3.8 ± 0.3
IRM	3.8 ± 0.2*	4.2 ± 0.5*	4.0 ± 1.4
LRM	2.5 ± 0.3	2.6 ± 0.2	2.4 ± 0.2
SRM	3.9 ± 0.3*	4.1 ± 0.5*	3.9 ± 1.1
SOM	2.6 ± 0.1	2.7 ± 0.5	2.6 ± 0.1
ON diameter	5.2 ± 0.2	5.3 ± 0.1	5.1 ± 0.2
ON length	27.5 ± 1.8	27.7 ± 0.8	27.4 ± 1.5
Anterior ethmoidal foramen			
LP-MRM	3.9 ± 0.3*	4.1 ± 0.9*	3.8 ± 0.7
LP-G	7.3 ± 0.5*	8.2 ± 0.1*	7.4 ± 0.9
LP-IRM	11.5 ± 0.4*	11.8 ± 1.7*	11.5 ± 0.3
LP-IOC	16.1 ± 1.2	16.2 ± 0.9	15.9 ± 0.1
Posterior ethmoidal foramen			
LP-MRM	0.5 ± 0	0.6 ± 0.1	0.5 ± 0.1
LP-ON	7.2 ± 0.9	7.3 ± 1.3	7.0 ± 0.1
LP-IRM	4.5 ± 0.7	4.7 ± 0.4	4.6 ± 1.1
LP-IOC	12.5 ± 0.3	12.6 ± 1.4	12.4 ± 1.3

MRM: medial rectus muscle, IRM: inferior rectus muscle, LRM: lateral rectus muscle, SRM: superior rectus muscle, SOM: superior oblique muscle, ON: optic nerve, LP: lamina papyracea, G: globe, IOC: infraorbital canal

Mean ± Standard Deviation; ANOVA test.

*indicates statistically significant p values ($p<0.05$).

Table 4: The distribution of the comparison in morphometric measurements between right and left sides

Extraocular muscle diameters (mm)	Right	Left	p value
	Mean ± SD	Mean ± SD	
MRM	3.9 ± 0.4	3.8 ± 0.5	0.425
IRM	3.9 ± 0.6	3.8 ± 0.7	0.432
LRM	2.5 ± 0.4	2.5 ± 0.6	0.879
SRM	4.1 ± 0.6	4.1 ± 0.7	0.887
SOM	2.5 ± 0.5	2.6 ± 0.5	0.21
ON diameter	5.3 ± 0.4	5.3 ± 0.4	0.954
ON length	27.7 ± 2.2	27.3± 2.3	0.557
Anterior ethmoidal foramen			
LP-MRM	4.0 ± 1.3	3.7 ± 1	0.058
LP-G	7.7 ± 1.4	7.8 ± 1.6	0.319
LP-IRM	11.7 ± 1.5	11.4 ± 1.6	0.485
LP-IOC	16.0 ± 2.1	16.3 ± 2	0.12
Posterior ethmoidal foramen			
LP-MRM	0.7 ± 0.4	0.5 ± 0.3	0.062
LP-ON	7.0 ± 1.8	7.4 ± 1.7	0.054
LP-IRM	4.8 ± 1.2	4.7 ± 1.3	0.449
LP-IOC	12.3 ± 2.4	12.6 ± 2.3	0.24

MRM: medial rectus muscle, IRM: inferior rectus muscle, LRM: lateral rectus muscle, SRM: superior rectus muscle, SOM: superior oblique muscle, ON: optic nerve, LP: lamina papyracea, G: globe, IOC: infraorbital canal; Mean ± Standard Deviation. Paired t test. $p<0.05$ shows statistically significant p values

RESULTS

The patients consisted of 23 females (43%) and 77 males (57%) with a median age of 48.60 ± 12.32 years for females and 37.36 ± 15.24 years for males. We divided the patients into 3 age groups; (1) group (18-39 y) including 94 orbits, (2) group (40-59 y) including 78 orbits, (3) group (60-90 y) including 28 orbits.

Extraocular muscles and optic nerve diameters

The mean values for the diameters of extraocular muscles and ON were given in Table 2. The mean horizontal diameters of the rectus muscles were measured as 3.9 ± 0.5 mm in medial, 2.5 ± 0.5 mm in lateral, 2.6 ± 0.5 mm in superior oblique, respectively. We reported that the mean vertical diameters of the rectus muscles were 4.1 ± 0.6 mm in inferior and 4.0 ± 0.6 mm in superior, respectively.

Also, the mean diameter and length of the ON were 5.3 ± 0.4 mm and 27.5 ± 2.2 mm. In Table 2, we demonstrated that all measurement values were higher in males than females and showed statistically significant differences except the diameter and length of the ON results. Also, these values showed significant differences with respect to aging (P<0.05) as seen in Table 3 but, there was no difference with respect to laterality (Table 4).

The distance measurements from medial wall of the orbit to intraorbital structures

We reported that the mean horizontal distances from LP to MRM, IRM, G and IOC at the depth of the AEF were 3.9 ± 1.2 mm, 11.5 ± 1.6 mm, 7.8 ± 1.5 mm and 16.1 ± 2.0 mm, respectively. In addition, at the depth of the PEF, the mean horizontal distances from LP to MRM, IRM, ON and IOC were measured as 0.6 ± 0.4 mm, 4.7 ± 1.3 mm, 7.2 ± 1.8 mm, 12.5 ± 2.3 mm, respectively. As seen in Table 2, the distances from the LP to the intraorbital structures including MRM, IRM, ON, G, and IOC were larger in males than females but not show statistically significant differences. The measurement results indicated that subjects in first and second age groups showed statistically significant differences in LP-MRM, LP-G and LP-IRM distances at the depth of AEF (p<0.05) as shown in Table 3, although there were no statistically significant differences between left and right.

DISCUSSION

The extraocular muscles, which lie from the orbital apex to the globe, can be damaged in several orbital pathologies including Graves' orbitopathy, tumors, and fractures. The increasing changes in extraocular muscle size can alter the globe position and are correlated to some orbital complications such as optic neuropathy, diplopia, and proptosis. Precise knowledge of normal diameters of the extraocular muscles is important in diagnosing, particularly in patients with Graves' disease, which mostly affects the superior rectus muscle (54.7%) and also used to check the treatment efficacy and the degree of proptosis [1,2,5,16-18]. To evaluate the dimensions of the extraocular muscles the CT or MRI can be used. By using MPR on CT scans, more accurate morphometric analysis can be done. The extraocular muscles can be seen as thin, well specified oval structures in the coronal plane of CT scans. Using coronal planes which is approximately 1 cm posterior to the globe all rectus muscles can be evaluated [1,16].

In previous studies, the diameters of the extraocular muscles were measured by using different imaging techniques as seen in Table 5 [1,2,5,16-19]. The discrepancies between measurement values may be related to the measurement technique, the plane which was used for measurement and ethnic differences. In addition, the lateral rectus muscles have more oblique course than other rectus muscles. So, its horizontal thickness measured in the coronal section may be slightly larger than that measured in the axial plane [1]. In our study, we measured the diameters of extraocular muscles and optic nerve at 1 cm posterior to the globe in the coronal plane, which the crista galli appeared. We reported that the mean horizontal diameters of the medial, lateral rectus and superior oblique muscles were 3.9 ± 0.5 mm, 2.5 ± 0.5 mm, and 2.6 ± 0.5 mm, respectively. Also, the mean vertical diameters of the inferior and superior rectus muscles were found as 4.1 ± 0.6 mm and 4.0 ± 0.6 mm, respectively. In addition, we measured the mean diameter and length of the ON as 5.3 ± 0.4 mm and 27.5 ± 2.2 mm. All measurement values, except the diameter and length of the ON, were higher in males than females as shown in Table 2. Although in Table 3, there were significant differences with respect to aging (P<0.05), there was no difference between right and left (Table 4). Because the measurements were performed in the same plane at the posterior aspect of the globe, our values were similar to the results of Shen et al. [1]. Also, the mean results of the previous studies and this study shows an increasing diameter of extraocular muscles from the inferior to the lateral rectus muscles as seen in Table 5 [1,2,5,16-19]. On the other hand, Lee et al. reported that all diameter values increased with aging but did not show statistically significant difference [1].

In view of endoscopic surgical approaches, there are many critical anatomic landmarks on the medial wall of the orbit, which adjoins with the paranasal sinuses. Because of the LP is extremely thin part (0.2-0.4 mm thick) of the medial wall, it can be fractured easily and also penetrated during endoscopic sinus surgery [20,21]. Also, during EEA, which is used for the reconstruction or removal of the retrobulbar pathologies, LP is mostly used. So, to know anatomic landmarks on the medial wall and its relationships with the intraorbital structures may increase the success rate of surgical operation and minimizes the iatrogenic complications [3,6,11,12]. Especially, the detailed understanding of the medial orbital anatomy including the AEF and PEF, which are key landmarks for the retrobulbar space and a safe compartment between the MRM and IRM guides a surgeon for appropriate surgical planning and a safe resection of intraorbital tumors [8-10,22]. The distances from the LP to the intraorbital structures such as ON, IOC, MRM, and IRM can provide important information about the surgeon's approximate location and prevent the iatrogenic neurovascular injury. Especially, during surgical interventions for the removal of retroorbital pathologies and posterior ethmoidectomy, the surgeon can specify a proper location and operate in a zone of confidence [3,6].

In literature, there was a few anatomic CT data of the orbit on the relationship between the extraocular muscles and LP, which may be important in helping to avoid orbital complications during surgery. Hwang et al. analyzed the CT scans of 100 patients and measured the distances from the medial orbital floor, which was a consistent anatomic landmark on ethmoidomaxillary suture, to intraorbital structures at the depth of the midportions of the anterior and posterior ethmoid sinuses [3]. They reported that the mean horizontal distances from the

medial orbital floor to MRM, IRM and IOC at the depth of the midportion of the anterior ethmoid sinus were 7.3 ± 1.4 mm, 9.0 ± 1.4 mm and 13.6 ± 1.6 mm, respectively. In addition, the mean horizontal distances from the medial orbital floor to MRM, IRM and IOC at the depth of the midportion of the posterior ethmoid sinus were 2.9 ± 0.9 mm, -0.9 ± 1.0 mm and 9.6 ± 1.2 mm, respectively [3]. Alternatively, we used the AEF and PEF, which represent the superior boundary of the ethmoidal roof, as a critical landmark on the LP in axial planes. Then, we measured the distances between the vertical axis passing along the LP and the intraorbital structures in coronal planes. In our study, we demonstrated that the mean horizontal distances from LP to MRM, IRM, G and IOC at the depth of the AEF were 3.9 ± 1.2 mm, 11.5 ± 1.6 mm, 7.8 ± 1.5 mm and 16.1 ± 2.0 mm, respectively. Also, at the depth of the PEF, the mean horizontal distances from LP to MRM, IRM, ON and IOC were measured as 0.6 ± 0.4 mm, 4.7 ± 1.3 mm, 7.2 ± 1.8 mm, 12.5 ± 2.3 mm, respectively. All values were larger in males than females but not show statistically significant differences as seen in Table 2. In Table 4, there was no difference with respect to laterality.

The volume of orbital fat increases with the aging, especially at the depth of the AEF, and affects the distances between the intraorbital structures and the medial wall of the orbit [3,4,12]. Hwang et al. demonstrated that the measurement values increased with respect to age depending on progressive intraorbital fat [3]. Similarly, we obtained that the mean measurement values showed a positive correlation in relation to age and indicated that subjects in first and second age groups showed statistically significant differences in LP-MRM, LP-G and LP-IRM distances at the depth of AEF ($p<0.05$) as shown in Table 3.

Compared with previous studies, our outcomes showed little diversity depending on the differences in reference landmarks, methodology, and ethnicities. On the other hand, using MPR images we measured some parameters which were not used in previous studies and useful for endoscopic surgery. So, the comparative data was deficient. Nevertheless, recruitment of the higher number of patients and future studies including measurements in children and patients with orbital pathology may give researchers more comprehensive results.

Table 5: The distribution of mean values of Extraocular muscle diameters in different studies

Extraocular Muscle Diameters						
Study	**MRM**	**IRM**	**LRM**	**SRM**	**SOM**	**ON**
Lee et al. (CT) [5]	3.7	4.1	3.4	4	-	4.3
Bulut et al. (CT) [17]	3.7	3.9	2.7	3.8	-	4.5
Lerdlum et al. (MDCT) [1]	3.7	4	3.6	3.8	-	-
Sheikh et al. (MDCT) [2]	4	4.8	3.4	4.7	-	-
Szucs-Farkas et al. (MRI) [16]	4.2	5.5	3.7	4.4	-	-
Bijlsma et al. (MRI) [19]	4	4.8	3.3	4.4	-	4.4
Shen et al. (MRI) [18]	3.9	4.7	2.3	4.3	2.4	5.4
This study (MDCT)	3.9	4.1	2.5	4	2.6	5.3

MRM: medial rectus muscle, IRM: inferior rectus muscle, LRM: lateral rectus muscle, SRM: superior rectus muscle, SOM: superior oblique muscle, ON: optic nerve.

CONCLUSIONS

We aimed to present the criteria for the diameters of healthy extraocular muscles and the ON, and their relationships with the LP in living CT scans. Also, we analyzed the effects of age, sex, and laterality on these parameter values. These results again emphasized the value of preoperative CT imaging which can offer an accurate understanding of the surgical anatomy of and around the LP. In conclusions, the detailed understanding of such surgical anatomic relationships in the medial compartment of the orbit in view of endoscopic approach can be of great help in appropriate surgical planning, meticulous dissection and predicting outcomes. As a result, the success of surgical technique increases and the postoperative complications can be decreased.

CONFLICT OF INTEREST

The authors' declares that they have no conflict of interest.

REFERENCES

1. Sukalaya Lerdlum MD, Boonsirikamchai P, Setsakol E. Normal measurements of extraocular muscle using computed tomography. J Med Assoc Thai 2007; 90:307-312.
2. Sheikh M, Abalkhail S, Doi SA, et al. Normal measurement of orbital structures: Implications for the assessment of Graves' ophthalmopathy. J Med Imaging Radiat Oncol 2007; 51:253-256.
3. Hwang SH, Park CS, Cho JH, et al. Anatomical analysis of intraorbital structures regarding sinus surgery using multiplanar reconstruction of computed tomography scans. Clin Exp Otorhinolaryngol 2013; 6:23.
4. Lee JM, Lee H, Park M, et al. The volumetric change of orbital fat with age in Asians. Ann Plast Surg 2011; 66:192-195.
5. Lee JS, Lim DW, Lee SH, et al. Normative measurements of Korean orbital structures revealed by computerized tomography. cta Ophthalmol Scand 2001; 79:197-200.
6. Lethaus B, Weigl S, Kloss-Brandstätter A, et al. Looking for landmarks in medial orbital trauma surgery. Int J Oral Maxillofac Surg 2013; 42:209-213.
7. Abuzayed B, Tanriover N, Gazioglu N, et al. Endoscopic endonasal approach to the orbital apex and medial orbital wall: Anatomic study and clinical applications. J Craniofac Surg 2009; 20:1594-1600.
8. Cankal F, Apaydin N, Acar HI, et al. Evaluation of the anterior and posterior ethmoidal canal

by computed tomography. Clin Radiol 2004; 59:1034-1040.
9. Celik S, Ozer MA, Kazak Z, et al. Computer-assisted analysis of anatomical relationships of the ethmoidal foramina and optic canal along the medial orbital wall. Eur Arch Otorhinolaryngol 2015; 272:3483-3490.
10. Karaki M, Kobayashi R, Kobayashi E, et al. Computed tomographic evaluation of anatomic relationship between the paranasal structures and orbital contents for endoscopic endonasal transethmoidal approach to the orbit. Oper Neurosurg 2008; 63:ONS15-ONS20.
11. Piagkou M, Skotsimara G, Dalaka A, et al. Bony landmarks of the medial orbital wall: An anatomical study of ethmoidal foramina. Clin Anat 2014; 27:570-577.
12. entokey.com/orbital-anatomy-and-its-clinical-applications/
13. Bleier BS, Healy Jr DY, Chhabra N, et al. Compartmental endoscopic surgical anatomy of the medial intraconal orbital space. Int Forum Allergy Rhinol 2014; 4:587-591.
14. Herzallah IR, Marglani OA, Shaikh AM. Variations of lamina papyracea position from the endoscopic view: A retrospective computed tomography analysis. Int Forum Allergy Rhinol 2015; 5:263-270.
15. Felding UA, Bloch SL, von Buchwald C. The dimensions of the orbital cavity based on high-resolution computed tomography of human cadavers. J Craniofac Surg 2016; 27:1090-1093.
16. Szucs-Farkas Z, Toth J, Balazs E, et al. Using morphologic parameters of extraocular muscles for diagnosis and follow-up of Graves' ophthalmopathy: Diameters, areas, or volumes? AJR Am J Roentgenol 2002; 179:1005-1010.
17. eskidergi.cumhuriyet.edu.tr/makale/202.pdf
18. Shen S, Fong KS, Wong HB, et al. Normative measurements of the Chinese extraocular musculature by high-field magnetic resonance imaging. Invest Ophthalmol Vis Sci 2010; 51:631-636.
19. Bijlsma WR, Mourits MP. Radiologic measurement of extraocular muscle volumes in patients with Graves' orbitopathy: A review and guideline. Orbit 2006; 25:83-91.
20. Hwang SH, Joo YH, Seo JH, et al. Endoscopic endonasal approach of the medial intraconal space: CT analysis of the anatomic relation between paranasal structures and orbital contents. J Craniofac Surg 2012; 23:966-969.
21. Suzuki M, Nakamura Y, Ozaki S, et al. Repair of orbital floor fracture with modified transnasal endoscopic approach through anterior space to nasolacrimal duct. J Craniofac Surg 2017; 28:998-1002.
22. McDonald SE, Robinson PJ, Nunez DA. Radiological anatomy of the anterior ethmoidal artery for functional endoscopic sinus surgery. J Laryngol Otol 2008; 122:264-267.